Improvement of DTI Measurement Accuracy Using Real-Time Navigated Data Acquisition

X. SHI[1], E. Kholmovski[2], S-E. Kim[2], D. L. Parker[2], and E-K. Jeong[2]

[1]Department of Physics, University of Utah, salt lake city, Utah, United States, [2]Department of Radiology, University of Utah, Salt Lake City, Utah, United States

INTRODUCTION Subject motion during the strong diffusion weighting (DW) gradient generally causes shading and ghosting artifacts in the resultant diffusion weighted images [1-3], and consequently results in reduced accuracy in the diffusion tensor imaging (DTI) measurement. Typically, DW images are acquired using singleshot acquisition methods such as 2D DWEPI with multiple averages to improve SNR. These motion artifacts may introduce inconsistency among the different averages. A Subject's physiological motion can be described as a translation followed by a rotation during the application of the diffusion gradient. Translational motion introduces an additional constant phase, while the rotational motion results in a shift of data in k-space which corresponds to a linear phase shift in image space [1, 2]. Both types of motion result in a significant signal loss, because even small motion can cause partial or complete dephasing. In this report, a motion artifact reduction scheme using real-time navigated (RTN) data acquisition is described for 2D singleshot DWEPI. In this technique, data with substantial motion corruption is identified and rejected/reacquired in real-time, using the realtime feedback capability of the pulse sequence.

METHODS RTN was implemented in a 2D singleshot diffusion weighted EPI pulse sequence (2D ss-RTN-DWEPI), by adding a realtime-feedback flag to all imaging echoes [3, 4]. An image reconstruction program was developed to process the 2D navigator echoes, which calculates the magnitude and the position of the largest echo peak, and sends these values to the scanning computer. The flowchart in Fig. 1 describes the procedure of the RTN data acquisition. If the amplitude and/or the position of the peak of the largest echo in the 2D navigator changes by more than 30% or shifts by more than 2 units of Δk compared to those of the reference navigator echoes, the scanner was instructed to reacquire the data. The first shot of each diffusion encoding direction was considered as the reference shot, because a subject may be more able to hold still in the earlier than in the later acquisitions.

DW imaging was performed on a 3 T clinical MRI system (Trio, Siemens Medical Solutions, Erlangen, Germany) with Sonata gradients (40 mT/m strength and 150 T/m/s slew rate) with common imaging parameters; slice thickness 2 mm and bandwidth 1.086 kHz/pixel. A cylindrical agarose phantom was imaged to test the feasibility of this real-time navigated technique with TR/TE 4000/60 ms, FOV 256x96 mm, acquisition matrix 128x48, and b values 0 and 500s/mm^2 along four diffusion encoding directions; (1,0,0), (0,0,1), (1,0,1), (-1,0,1). The phantom was intermittently moved during imaging to simulate physiological motion. A phase image was reconstructed by the method described in Fig. 2. 2D ss-RTN-DWEPI was also applied to a healthy human brain using TR/TE 5000/66 ms, FOV 256x192 mm, acquisition matrix 128x96, and b = 0 and 750 s/mm^2 in 7 non-collinear directions; (1,0,0), (0,1,0), (0,0,1), (1,1,1), (-1,-1,1), (1,-1,-1), (-1,1,-1).

RESULTS and DISCUSSION Phantom images are shown in Fig. 3. The corrupted shot in the second diffusion encoding direction (Fig. 3a-2 enclosed by solid circle) was reacquired. The quality of the magnitude and phase in the reacquired shot (Fig. 3a-2 enclosed by dotted circle) was greatly improved by RTN. For multiple slice imaging, the comparison was performed slice by slice. For instance, in the third diffusion encoding direction, although the magnitude and the phase images of slice 6 were not corrupted, the measurements was repeated because the images of slice 0 and 2 were corrupted in the same shot as in Figs. 3b and 3d. The numbers enclosed by rectangular boxes indicate the slice numbers. In Fig. 4a, an obvious shading artifact is shown in the human brain image. Signal intensity was greatly changed. The phase image (Fig. 4b) is completely distorted. The magnitude and phase images of the reacquired shot were greatly improved as in Figs. 4c and 4d.

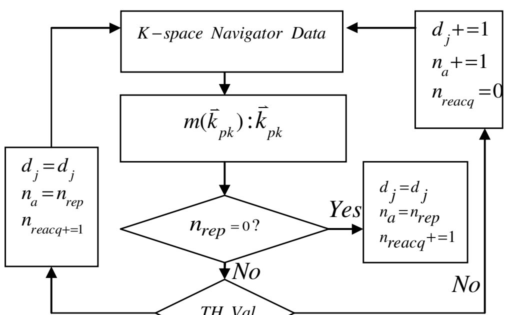

Threshold Value(*TH.Val.*) :

$$\left|m(\bar{k}_{pk},d_j)-m(\bar{k}^0_{pk},d_j)\right|/m(\bar{k}^0_{pk},d_j)>0.3$$

$$Or\left|\bar{k}_{pk}-\bar{k}^0_{pk}\right|>2 \; and \; n_{reacq}<4$$

Figure 1: Flowchart of RT navigated acquisition. 2D navigator echoes are sent to the reconstruction computer to calculate the magnitude and the position of the largest echoes. These values are transferred to the scan computer to determine if the data is acceptable compared to the first repetition data. It is assumed that human subjects may move less in early repetitions than the later acquisitions. The indices d_j, n_a, and n_{reacq} are the diffusion direction, average counter, and reacquisition counter, respectively.

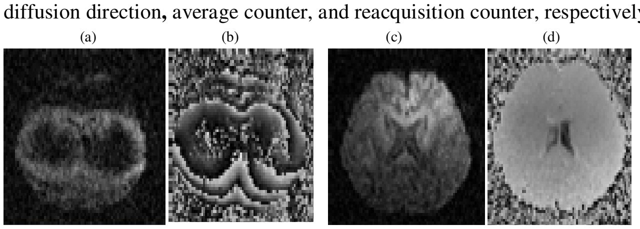

Figure 4: Motion corrupted magnitude image (a) and corresponding phase image (b) of a human brain. Reacquired magnitude image (c) and the corresponding phase image (d).

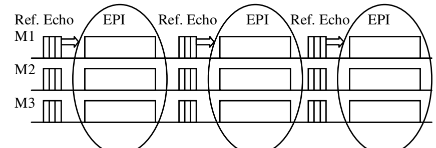

Figure 2: Under the same experimental condition, three measurements (M1, M2 and M3) are acquired. Assuming that the subject experiences no motion during the first measurement, three reference echoes of the first measurement M1 were used to correct all the corresponding EPI data in the following measurements, M2 and M3.

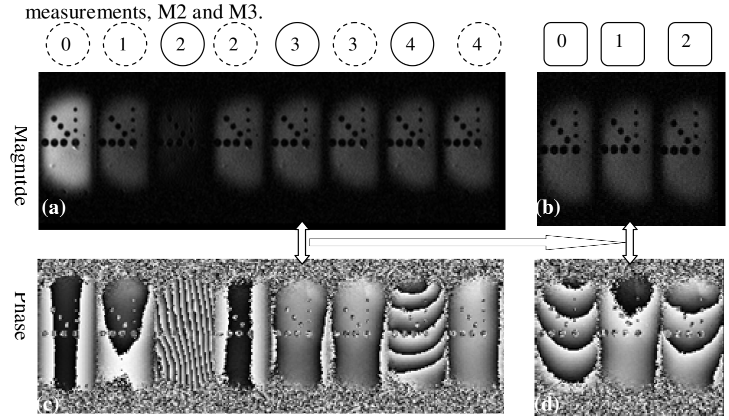

Figure 3: Motion corrupted magnitude (a) and phase (c) images of slice 6 in different diffusion encoding direction are compared to those of motion free reference (the first shot). Dotted and solid circles indicate the accepted and the rejected measurements, respectively. (b) and (d) represents the magnitude and phase images of 3 different slices of the current shot in the 3rd diffusion gradient encoding. The rectangular boxes with different numbers represent different slices in a specific measurement.

ACKNOWLEDGEMENTS: This work was supported by Cumming Foundation, NIH grants R21NS052424, R21EB005705, and R01HL57990, the Benning Foundation, and the Mark H. Huntsman Endowment.

REFERENCES: [1] Ordidge RJ, et al. MRI 1994;12:455-60. [2] Pipe JG, et al. MRM 2002;47:42-52. [3] XF Shi, et al. In: Proceeding of the 14th Annual Meeting of ISMRM, Seattle, Washington, USA, 2006, p2982. [4] EK Jeong, et al. MRM 2005;54(6):1575-1579.